New Model for Activation of Yeast Pyruvate Decarboxylase by Substrate Consistent with the Alternating Sites Mechanism: Demonstration of the Existence of Two Active Forms of the Enzyme†

Eduard A. Sergienko*,‡ and Frank Jordan*

Department of Chemistry and Program in Cellular and Molecular Biodynamics, Rutgers, The State University of New Jersey, Newark, New Jersey 07102

Received September 28, 2001; Revised Manuscript Received January 2, 2002

ABSTRACT: Pyruvate decarboxylase from yeast (YPDC, EC 4.1.1.1) exhibits a marked lag phase in the progress curves of product (acetaldehyde) formation. The currently accepted kinetic model for YPDC predicts that, only upon binding of substrate in a regulatory site, a slow activation step converts inactive enzyme into the active form. This allosteric behavior gives rise to sigmoidal steady-state kinetics. The E477Q active site variant of YPDC exhibited hyperbolic initial rate curves at low pH, not consistent with the model. Progress curves of product formation by this variant were S-shaped, consistent with the presence of three interconverting conformations with distinct steady-state rates. Surprisingly, wild-type YPDC at pH ≤5.0 also possessed S-shaped progress curves, with the conformation corresponding to the middle steady state being the most active one. Reexamination of the activation by substrate of wild-type YPDC in the pH range of 4.5−6.5 revealed two characteristic transitions at all pH values. The values of steady-state rates are functions of both pH and substrate concentration, affecting whether the progress curve appears "normal" or S-shaped with an inflection point. The substrate dependence of the apparent rate constants suggested that the first transition corresponded to substrate binding in an active site and a subsequent step responsible for conversion to an asymmetric conformation. Consequently, the second enzyme state may report on "unregulated" enzyme, since the regulatory site does not participate in its generation. This enzyme state utilizes the alternating sites mechanism, resulting in the hyperbolic substrate dependence of initial rate. The second transition corresponds to binding a substrate molecule in the regulatory site and subsequent minor conformational adjustments. The third enzyme state corresponds to the allosterically regulated conformation, previously referred to as activated enzyme. The pH dependence of the Hill coefficient suggests a random binding of pyruvate in a regulatory and an active site of wild-type YPDC. Addition of pyruvamide or acetaldehyde to YPDC results in the appearance of additional conformations of the enzyme.

Pyruvate decarboxylase (EC 4.1.1.1) catalyzes the non-oxidative decarboxylation of pyruvate to acetaldehyde (Scheme 1) and requires thiamin diphosphate (ThDP)[1] and Mg(II) as cofactors. Yeast pyruvate decarboxylase (YPDC) from *Saccharomyces cerevisiae* is an enzyme consisting of four identical subunits with the ThDP bound at the interface created by two subunits forming a tight dimer (*1*, *2*). Two of these dimers form a loose tetramer usually described as a "dimer of dimers".

Pyruvate decarboxylases from all sources, except *Zymomonas mobilis* (ZmPDC), exhibit allosteric activation by the substrate pyruvate (*3*) or the substrate analogue pyruvamide (*4*). This activation is believed to entail a slow conformational change involving the entire enzyme molecule. Progress curves of product formation exhibit a pronounced lag phase, attributed to a change of activity from zero of the unregulated enzyme conformation to the steady-state value of the activated enzyme. The v_0−[S] plots exhibit pronounced sigmoidal behavior, formerly explained through a compulsory binding of the substrate in the regulatory site prior to its binding in the active site. In a series of contributions from this laboratory, evidence has been presented indicating that C221 on the β domain is the site where the regulatory pyruvate molecule is first bound, and this event generates the signal which is then transmitted to the ThDP cofactor located between the α and the γ domains (*5*−*13*). So far, this signal pathway is also believed to include H92, E91, W412, and likely (although not tested so far) G413, which forms one of three highly conserved hydrogen bonds to the ThDP, specifically to the N4′-amino group.

Our interest in a reexamination of the activation mechanism (as contrasted with the pathway) was kindled by our

† Supported by NIH Grant GM50380 and Roche Diagnostics Corp., Indianapolis, IN.

* To whom correspondence should be addressed. E.A.S.: e-mail, esergienko@triadt.com. F.J.: tel, 973-353-5470; fax, 973-353-1264; e-mail, frjordan@andromeda.rutgers.edu.

‡ Current address: Triad Therapeutics, San Diego, CA 92121.

[1] Abbreviations: ThDP, thiamin diphosphate; ADH, alcohol dehydrogenase (yeast); BFD, benzoylformate decarboxylase; WT YPDC, wild-type yeast pyruvate decarboxylase from *Saccharomyces cerevisiae* overexpressed in *Escherichia coli*; E477Q, D28A, and D28N, variants of this enzyme with the indicated substitutions; ZmPDC, pyruvate decarboxylase isolated from *Zymomonas mobiliz.*

10.1021/bi011860a CCC: $22.00
Published on Web 03/03/2002

Scheme 1

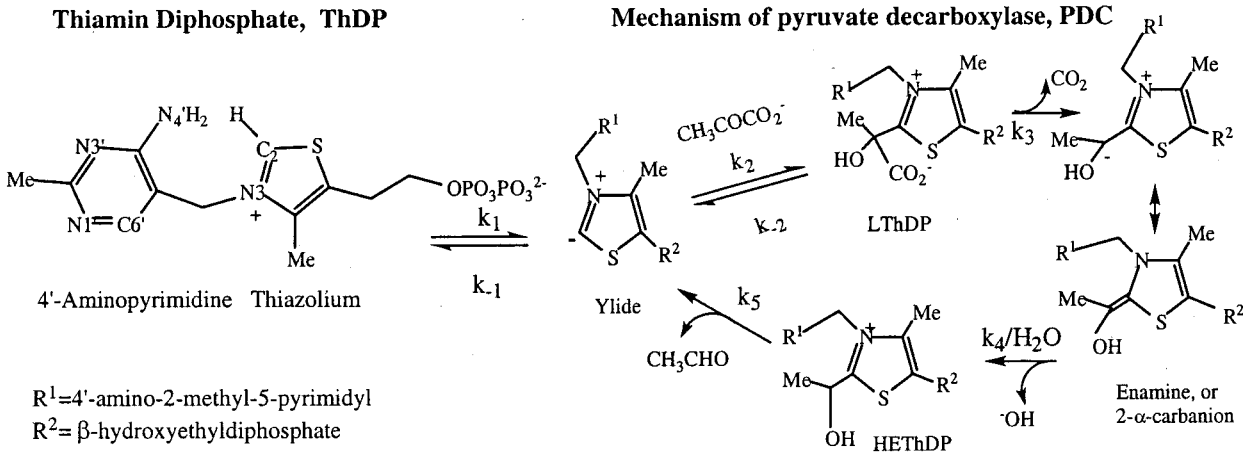

Scheme 2: Full Scheme of Alternating Sites Mechanism

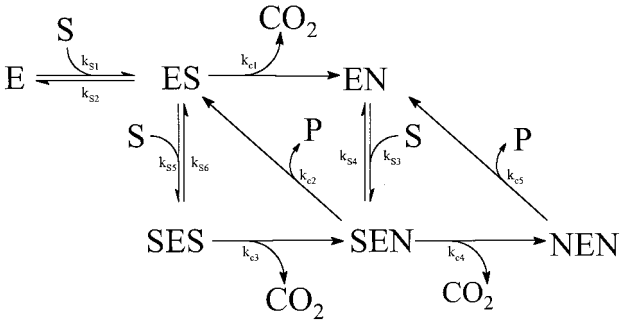

Scheme 3: Simplified Version of Alternating Sites Mechanism of WT YPDC

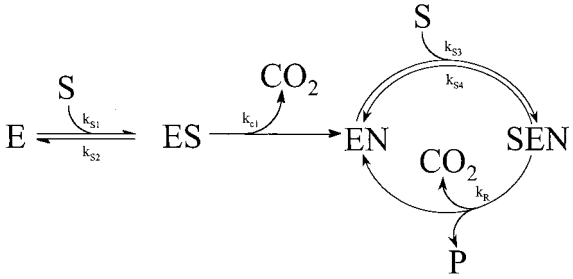

recent studies carried out on the steady-state behavior of YPDC variants (*14*−*16*), with substitutions at the active center D28, H114, H115, and E477 residues. Along with steady-state kinetic data of the principal acetaldehyde-forming reaction, results were also reported for the D28A, D28N, and E477Q variants undergoing the so-called carboligase reactions forming acetoin and acetolactate. The sum of the observations necessitated the formulation of a new kinetic model with alternating active sites (*16*), such that the minimal catalytic unit of YPDC is a "functional dimer" corresponding in structure to the tight dimer mentioned above. This dimer utilizes its active sites in an ordered fashion (Scheme 2, where E represents activated enzyme). According to the model, product release in one active site of WT YPDC under optimal conditions is tightly coupled to the decarboxylation step in the second active site of the functional dimer. A simplified version of the model is shown in Scheme 3, where steps responsible for activation and inhibition are omitted and both decarboxylation and product release are denoted by a single arrow (k_R). This condition requires that WT YPDC exist nearly exclusively as one of only two species labeled EN and SEN. The EN represents functional dimer with one active site occupied with a postdecarboxylation intermediate and the second site empty. The SEN represents functional dimer with both active sites occupied, one by a predecarboxylation intermediate (SE part) and the other by a postdecarboxylation intermediate (EN part).

Substitution at the active site of YPDC accentuated the intrinsic parts of the single mechanism, slowing down individual steps and accumulating some covalent intermediates that would otherwise be present at only negligible concentrations. This allowed us to observe the appearance of several features not observable with the WT YPDC, one being a hyperbolic v_0−[S] plot for the E477Q variant at pH 5.0. We explained this observation by assuming that unregulated enzyme (i.e., enzyme species prior to formal activation) has activity equal to that of activated enzyme, making the binding of substrate in the regulatory site inconsequential. The alternative explanation suggested that the E477Q variant at low pH is indeed in the activated form; however, the substrate-binding step responsible for activation is invisible due to kinetic reasons. This invisibility of the activation step at this pH could result from the regulatory site of the E477Q variant having a much higher affinity for pyruvate than does the active site. The invisibility of the binding in the regulatory site could also result from a separation of the binding step from the catalytic cycle by an irreversible step. The E477Q substitution in the active site of YPDC resulted in slow product release, leading to the accumulation of enamine intermediate (NEN in Scheme 2). Under these conditions, the most populated catalytic pathway of the variant under steady-state conditions is the cycle EN → SEN → NEN → (EN), which is separated from the free enzyme pool by a chemically and phenomenologically irreversible decarboxylation step. The two alternative mechanisms leading to invisibility of the usually present activation process should display different pre-steady-state kinetics, reflecting on the path from the free enzyme to the predominant steady-state species. The extremely low activity of the variant, especially at low pH (*14*), complicates the analysis. Also, one may have questioned whether the conclusions reached about regulation would apply to the WT YPDC, given that the substitution is in the active site.

On the other hand, if the additional transition is a result of the alternating sites mechanism, such anomalies should be evident even in the pre-steady-state kinetic behavior of WT YPDC. The alternating sites mechanism is based on tight communication between active sites of the functional dimer, with the ionizable residues D28, E477, and H115 likely to be important in creating this communication, which in turn probably results in a strong pH effect on regulation. We therefore undertook a thorough study of the pH dependence of activation of WT YPDC and here present detailed analysis of the substrate-dependent activation process in the pH range of 4.5−6.5. Surprisingly, at low pH, WT YPDC gave rise to an S-shaped progress curve, implying the presence of three apparent steady-state rates (also implying the presence of three distinct states or conformations),[2] with the intermediate enzyme state being the most active one. This intermediate enzyme state has never been observed previously, and to fill this gap in our understanding of the YPDC mechanism, we characterized this conformation in greater detail. With a change of pH, the relative concentrations of the three conformations changed; however, their very existence even at pH 6.0 was beyond a doubt. This work therefore presents a more complicated picture for substrate activation of YPDC than heretofore accepted. The work further supports our contention that this enzyme remains a very important one as a model for enzyme regulation in general.

EXPERIMENTAL PROCEDURES

Materials. NADH was purchased from Sigma, St. Louis, MO. ADH was from Biozyme Laboratories, San Diego, CA. All other reagents were of analytical grade or higher.

Purification of the YPDC variants was described in the earlier papers (*14*, *15*). Holoenzymes of the variants and WT YPDC were utilized in all experiments.

Determination of the Pre-Steady-State Kinetic Parameters. The progress curves of product (acetaldehyde) formation were recorded via a yeast alcohol dehydrogenase/NADH coupled assay (*17*) on an Applied Photophysics SX18 MV stopped-flow spectrophotometer (Leatherhead, U.K.). A triple pH buffer consisting of 50 mM acetic acid, 50 mM MES, 100 mM Tris, 5 mM $MgCl_2$, and 0.5 mM ThDP was utilized in all pH-dependent kinetic experiments to ensure a constant ionic strength (*18*). Pyruvate decarboxylase (wild type, 10−84 μg/mL or 0.17−1.43 μM active sites; E477Q variant, 0.47 mg/mL or 7.8 μM) was premixed with NADH (0.3 mM) and ADH (350 units/mL). This solution was then mixed in a 1:1 ratio with pyruvate at different concentrations dissolved in the same buffer. The temperature was maintained at 31 °C with a Lauda MGW water bath. The absorbance change at 340 nm was measured with a light path of either 2 or 10 mm. The data (total of 4000 points) were transferred to a PC and treated with the SigmaPlot software according to the equation:

$$P = \frac{k_{tr2}(v_2 - v_0) + k_{tr1}(v_0 - v_1)}{k_{tr1}(k_{tr1} - k_{tr2})}(1 - e^{-k_{tr1}t}) + \frac{(v_1 - v_2)k_{tr1}}{(k_{tr1} - k_{tr2})k_{tr2}}(1 - e^{-k_{tr2}t}) + v_2 t \quad (1)$$

where v_0, v_1, and v_2 depict activities of three distinct enzyme states, E_0, E_1, and E_2. The rate constant k_{tr1} pertains to the transition from E_0 to E_1 and k_{tr2} to the transition from E_1 to E_2. When we wished to compare the results with those given by the earlier model involving just two enzyme states, eq 2 was used:

$$P = \frac{v_0 - v_1}{k_{tr1}}(1 - e^{-k_{tr1}t}) + v_1 t \quad (2)$$

where all parameters have the same meaning as in eq 1. Equation 2 can be obtained from eq 1 by setting $v_1 = v_2$.

Quenching of the Intrinsic YPDC Fluorescence in the Presence of Pyruvate. Stopped-flow fluorescence experiments were carried out on an Applied-Photophysics instrument (295 nm excitation wavelength with an optical filter with a cutoff at 305 nm). WT YPDC was diluted to a concentration of 0.4 mg/mL in the triple buffer at pH 4.5 containing 5 mM $MgCl_2$ and 1 mM ThDP. It was then mixed at a 1:1 ratio with various concentrations of pyruvate dissolved in the same buffer. Time-dependent fluorescence changes were measured at 31 °C.

Circular Dichroism Kinetic Studies of the Rate of Acetoin Formation by the E477Q Variant. The YPDC variant (0.194 mg/mL) was dissolved in a pH buffer consisting of 50 mM acetic acid and 100 mM MES (pH 5.1) and also containing 5 mM $MgCl_2$ and 0.1 mM ThDP. It was either added to the reaction mixture containing 10 mM pyruvate and 50 mM acetaldehyde or preincubated for 5 min with 10 mM pyruvate (giving negligible ellipticity changes), followed by the addition of 50 mM acetaldehyde. The formation of acetoin was measured at 280 nm at 25 °C on an AVIV Model 202 CD instrument (AVIV Instruments, Inc.) as described elsewhere (*15*). The molar ellipticity of acetoin produced by the E477Q variant at pH 5.1 is 36.4 deg M^{-1} cm^{-1} (*15*).

RESULTS

Pre-Steady-State Kinetics of the E477Q Variant at pH 5.1. The E477Q variant displayed the usual activation kinetics during the initial 5−10 s of the progress curves (inset to Figure 1). However, the progress curve leveled off to a slower steady-state rate after 20−30 s, resulting in the appearance of the curve with an inflection point shown in Figure 1 (henceforth called an S-shaped curve). The data presented in the figure were treated according to eq 1, describing an interconversion of three conformations with distinguishable steady-state rates. The activity of the first state, E_0, appears to be zero (see inset to Figure 1), of the second state, E_1, it is 0.14 unit/mg, and of the third state, E_2, it is 0.068 unit/mg. The rate constants calculated for the transitions were $k_{tr1} = 0.66$ s^{-1} and $k_{tr2} = 0.031$ s^{-1}.

pH-Dependent Pre-Steady-State Kinetics of the WT YPDC. At low pH values the shape of the curve was similar to the one observed for the E477Q variant, revealing the presence of three distinct enzyme states. At higher pH, the shape of the progress curves resembled the one reported earlier (*4*); however, nonlinear regression analysis definitively indicated

[2] Throughout this paper, the authors will refer to E_0, E_1, and E_2 as the three states (or conformations, a term used interchangeably) reported on by the three steady-state rates v_0, v_1, and v_2. The difference among these states (conformations) may be very subtle, as simple as the presence of a substrate either in a regulatory or in an active site. The key issue is that they are kinetically distinguishable.

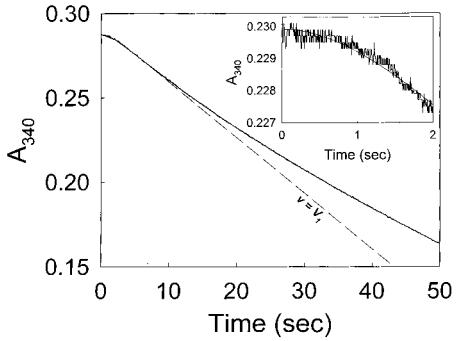

FIGURE 1: Progress curve for acetaldehyde formation by the E477Q YPDC variant. Enzyme (0.47 mg/mL) dissolved in 50 mM acetic acid and 100 mM MES, pH 5.1, containing 350 units/mL ADH, 0.12 mM NADH, 10 mM $MgCl_2$, and 1 mM ThDP was mixed in a 1:1 ratio with 20 mM pyruvate in the same buffer. The temperature was maintained at 31 °C. Absorbance changes were measured at 340 nm. The resulting progress curve was fitted to eq 1. The values of the parameters are $v_0 = 0$, $v_1 = 0.14$ units/mg, $v_2 = 0.068$ units/mg, $k_{tr1} = 0.66$ s^{-1}, and $k_{tr2} = 0.031$ s^{-1}. The dashed curve represents the linear portion with slope equal to v_1.

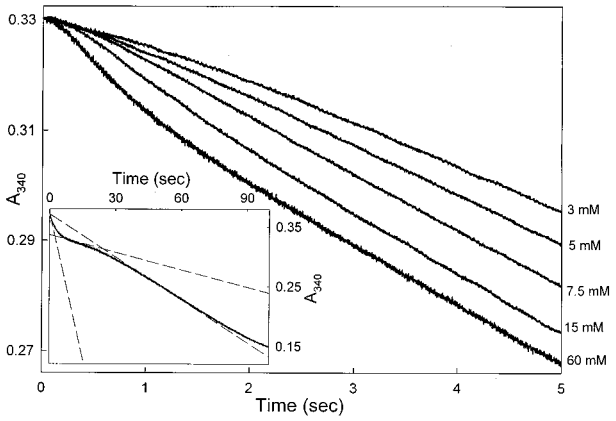

FIGURE 2: Progress curves for acetaldehyde formation by WT YPDC at different concentrations of pyruvate. WT YPDC (21 μg/mL) dissolved in triple buffer, pH 5.0, containing 350 units/mL ADH, 0.3 mM NADH, 10 mM $MgCl_2$, and 1 mM ThDP was mixed in a 1:1 ratio with solutions of pyruvate at different concentrations to give the final concentrations shown in the figure. Inset: Conditions are the same as in the main figure, except WT YPDC (42.2 μg/mL) was dissolved at pH 4.5 and the final concentration of pyruvate is 100 mM. Dashed lines represent tangent lines at the inflection points.

the presence of three steady-state rates. The shape of the observed curves depended on both pyruvate concentration (Figure 2) and pH (Figure 3) in a mutually interdependent manner. That is, the shape of the curve changed from "normal" (as observed for WT YPDC at pH 6.0) to the S-shaped behavior, and the pH of the transition depended on substrate concentration and vice versa. For example, at 30 mM pyruvate the rates v_1 and v_2 are equal at pH 5.2, whereas at 7.5 mM pyruvate the two rates are equal near pH 5.0. The higher the concentration of pyruvate, the higher the pH where the S-shaped curve changes to the normal one. Remarkably, additional transitions could be observed at pH 4.5 in the presence of pyruvate at concentrations >30 mM, preventing us from using those progress curves (inset to Figure 2).

The progress curves were treated according to eq 1 with the assumption that three enzyme conformations, E_0, E_1, and E_2, with corresponding distinct steady-state rates (v_0, v_1, and

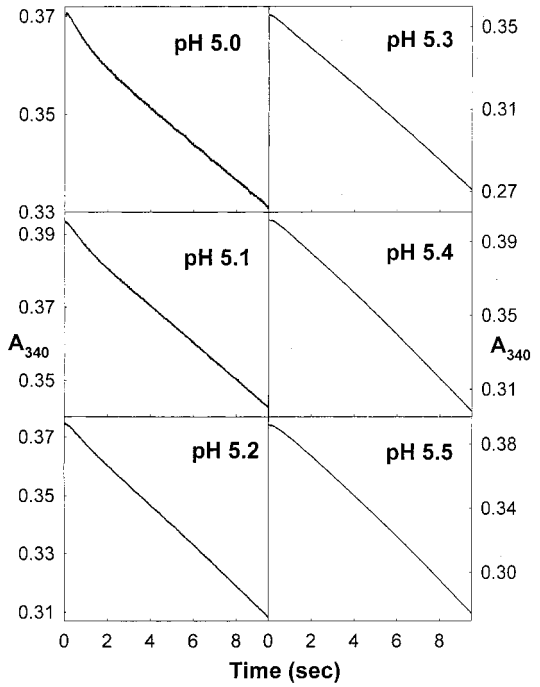

FIGURE 3: Progress curves for acetaldehyde formation by WT YPDC at different pH values. WT YPDC (10.5 μg/mL) dissolved in triple pH buffer at the indicated pH values, containing 350 units/mL ADH, 0.3 mM NADH, 5 mM $MgCl_2$, and 1 mM ThDP, was mixed in a 1:1 ratio with a solution of 60 mM pyruvate.

Scheme 4: Two-Step Phenomenological Model of YPDC Activation

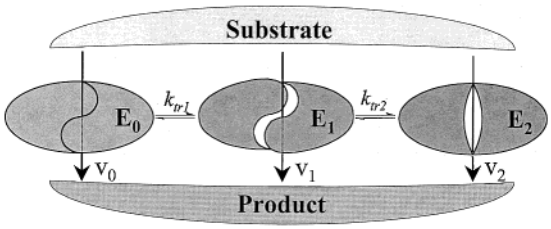

v_2) undergo consecutive transitions ($E_0 \rightarrow E_1 \rightarrow E_2$) as shown in Scheme 4. The resulting parameters at pH 4.5, 5.0, and 6.0 are shown in Figures 4, 5, and 6, respectively. The parameters at pH 5.0 have much larger errors due to similar values of v_1 and v_2, especially at low concentrations of substrate, resulting in the progress curve being almost linear.

The value of the first steady-state rate v_0 was negligible compared with the other two at all pH values (see inset to Figure 4A) and therefore was set to zero for all pH values. Both subsequent steady-state rates (v_1 and v_2) have nonzero values; these displayed saturation with substrate, and their relative values were a function of both pH and substrate concentration.

The rate v_1 vs [pyruvate] curve exhibited hyperbolic behavior at all pH values. Both K_m and V_{max} increased with increasing pH (Table 1). The rate of the third steady-state v_2 displayed sigmoidal substrate dependence. Not only V_{max} and $S_{0.5}$ but also n_H was a function of pH, and all three parameters increased with increasing pH (Table 2). At pH 4.5, the n_H is 0.72 and increases to 1.43 at a pH of 6.5. Surprisingly, the V_{max} of the E_2 state was lower than that of the E_1 state at all pH values. But, the half-maximal concentration of pyruvate ($S_{0.5}$) was always lower in the E_2 state than in the E_1 state. This condition, and the presence

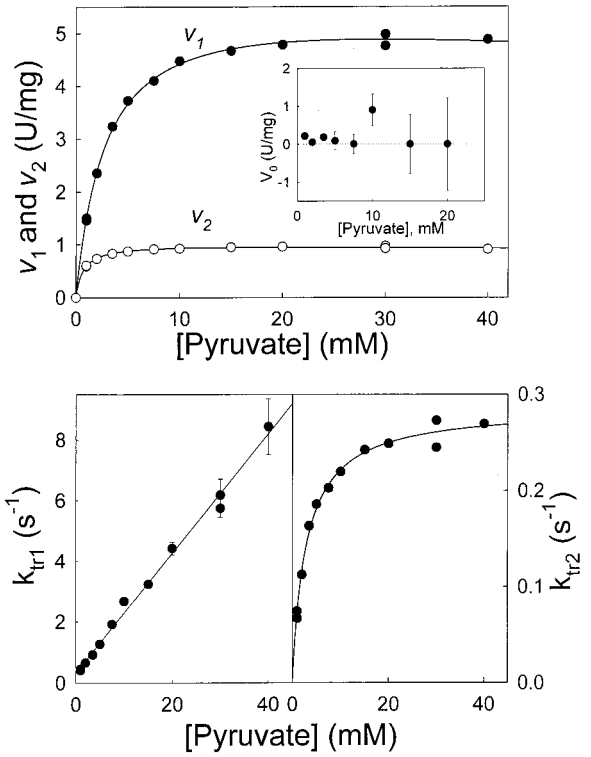

FIGURE 4: Parameters of the activation process at pH 4.5. All conditions are as in the inset to Figure 2. The progress curves for acetaldehyde formation were fitted to eq 1. The values of v_1 and v_2 were fitted to hyperbolic and Hill equations; the values k_{tr1} and k_{tr2} were fitted with linear and hyperbolic equations with an offset. Solid curves represent the best fit with the following parameters: (v_1) $V_{max} = 5.85$ units/mg and $K_m = 2.88$ mM; (v_2) $V_{max} = 1.14$ units/mg, $S_{0.5} = 0.86$ mM, and $n_H = 0.72$; (k_{tr1}) $k_1 = 0.197$ mM^{-1} s^{-1} and $k_{-1} = 0.32$ s^{-1}; (k_{tr2}) $k_2 = 0.29$ s^{-1}, $K_{d2} = 2.9$ mM, and $k_{-2} = 0.0$ s^{-1}.

Table 1: Kinetic Parameters of the Second Conformation (E_1) for Wild-Type YPDC

pH	k_{cat} (s^{-1})	K_m (mM)	k_{cat}/K_m (mM^{-1} s^{-1})
4.5	5.85 ± 0.13	2.88 ± 0.15	2.03
5.0	54.5 ± 5.7	32.5 ± 5.9	1.68
5.5	63.1 ± 3.1	28.6 ± 2.0	2.21
6.0	80.5 ± 12.2	23.4 ± 5.3	3.44
6.5	178.7 ± 43.2	83.4 ± 23.5	2.14

Table 2: Kinetic Parameters of the Third Conformation (E_2) for Wild-Type YPDC

pH	k_{cat} (s^{-1})	$S_{0.5}$ (mM)	n_H	$k_{cat}/S_{0.5}^n$	$k_{cat}/S_{0.5}$ (mM^{-1} s^{-1})
4.5	1.14 ± 0.08	0.86 ± 0.15	0.72 ± 0.12	1.27	1.33
5.0	12.5 ± 0.5	2.54 ± 0.43	1.00[a]	4.92	4.92
5.5	44.1 ± 0.6	2.36 ± 0.06	1.27 ± 0.04	14.82	18.68
6.0	50.6 ± 2.0	3.03 ± 0.23	1.37 ± 0.12	11.08	16.70
6.5	63.1 ± 1.0	4.79 ± 0.15	1.43 ± 0.04	6.72	13.17

[a] The parameter was fixed to the presented value.

of more pronounced inhibition by substrate in the E_1 state, resulted in $v_1 < v_2$ at all pyruvate concentrations utilized for pH >5.0 (see, for example, Figure 6).

The first transition ($E_0 \rightarrow E_1$) was characterized by an apparent rate constant (k_{tr1}) linearly dependent on pyruvate concentration, suggesting that this transition corresponds to a substrate-binding step. The slope of the line is equal to

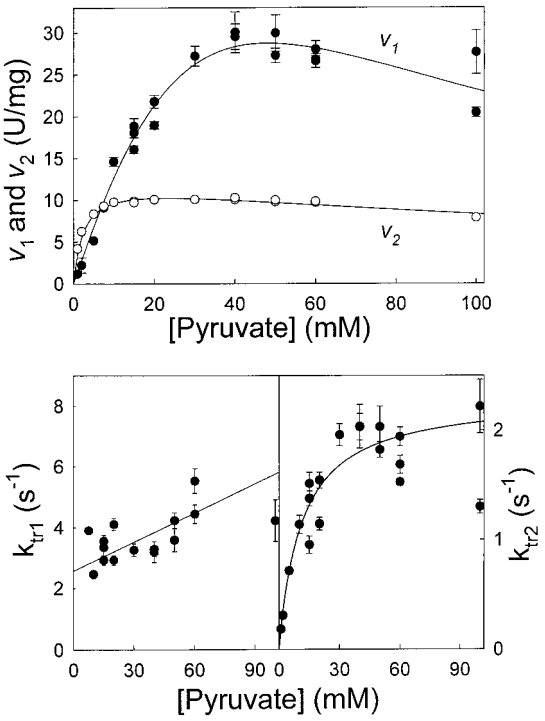

FIGURE 5: Parameters of the activation process at pH 5.0. All conditions are as in Figure 2. The progress curves for acetaldehyde formation were fitted to eq 1. The values of v_1 and v_2 were fitted to a hyperbolic equation and the values k_{tr1} and k_{tr2} to linear and hyperbolic equations with an offset.

the second-order rate constant for the enzyme−pyruvate complex formation k_1 (first order in substrate), while the intercept on the positive ordinate corresponds to the rate constant for dissociation of the complex k_{-1}. The ratio of the two rate constants k_{-1}/k_1 represents the dissociation constant K_{d1} of the complex. Only k_1 exhibited a pronounced dependence on pH, with a monotonic decrease with increasing pH (Table 3), and as a result, K_{d1} increased with increasing pH, changing from 1.6 to 62 mM with a pH increase from 4.5 to 6.5.

The second transition exhibited hyperbolic saturation of the apparent rate constant with increasing pyruvate concentration. Therefore, this transition corresponds to a step after enzyme−substrate complex formation. The fit to the hyperbolic equation with an offset (eq 3) resulted in values for k_2

$$k_{tr2} = \frac{k_2[S]}{K_{d2} + [S]} + k_{-2} \qquad (3)$$

and k_{-2}, the on- and off-rate constants for complex formation, and K_{d2}, the dissociation constant of the complex. The rate constant k_2 was virtually pH independent at pH >5.0 (Table 3), while k_{-2} values are very small compared to those of k_2 and therefore have a large associated error. The values of K_{d2} increased with increasing pH, changing from 2.9 to 33 mM (Table 3).

Fluorescence Changes on Addition of Pyruvate or Pyruvamide to WT YPDC. Addition of pyruvate to YPDC resulted in significant and rapid changes in intrinsic fluorescence (Figure 7A). At low pyruvate concentrations, a rapid fluorescence change was preceded by an initial lag phase and then followed by a slow steady-state decrease after prolonged time (data not shown). The changes in fluores-

Table 3: Parameters of the YPDC Activation Transitions

	first transition ($E_0 \rightarrow E_1$)			second transition ($E_1 \rightarrow E_2$)		
pH	k_1 ($M^{-1} s^{-1}$)	k_{-1} (s^{-1})	K_{d1} (mM)	k_2 (s^{-1})	k_{-2} (s^{-1})	K_{d2} (mM)
4.5	197.3 ± 5.1	0.32 ± 0.10	1.61	0.29 ± 0.01	0.00[a]	2.9 ± 0.2
5.0	31.8 ± 9.13	2.57 ± 0.34	80.6	2.31 ± 0.18	0.00[a]	11.3 ± 3.2
5.5	43.6 ± 2.6	1.11 ± 0.13	25.5	0.69 ± 0.05	0.01 ± 0.01	8.5 ± 1.1
6.0	16.4 ± 0.8	0.52 ± 0.03	31.6	0.69 ± 0.38	0.02 ± 0.04	20.3 ± 15.3
6.5	8.64 ± 0.58	0.54 ± 0.03	62.0	0.61 ± 0.13	0.03 ± 0.01	33.7 ± 11.7

[a] The parameter was fixed to the presented value.

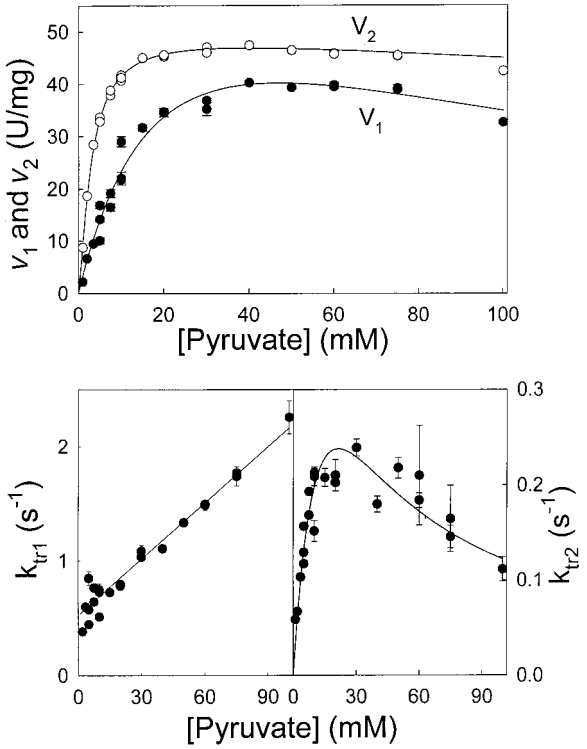

FIGURE 6: Parameters of the activation process at pH 6.0. The progress curves for acetaldehyde formation at pH 6.0 were fitted to eq 1. All conditions are as in Figure 2 except WT YPDC concentration was 5.3 μg/mL. The values of v_1 and v_2 were fitted to hyperbolic and Hill equations and the values k_{tr1} and k_{tr2} to linear and hyperbolic equations with an offset. Solid curves represent the best fit with the following parameters: (v_1) V_{max} = 82.1 units/mg, K_m = 24.0 mM, and K_i = 87.6 mM; (v_2) V_{max} = 50.6 units/mg, $S_{0.5}$ = 3.03 mM, and n_H = 1.37; (k_{tr1}) k_1 = 16.4 M^{-1} s^{-1} and k_{-1} = 0.52 s^{-1}; (k_{tr2}) k_2 = 0.69 s^{-1}, K_{d2} = 20.3, K_i = 22.5 mM, and k_{-2} = 0.03 s^{-1}.

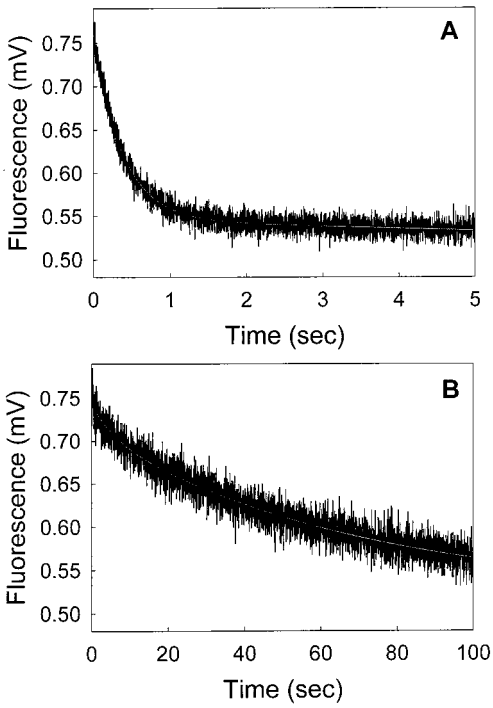

FIGURE 7: Fluorescence quenching in WT YPDC on addition of pyruvate (A) and pyruvamide (B). Enzyme at a concentration of 0.4 mg/mL dissolved in the triple pH buffer, pH 4.5, 5 mM $MgCl_2$, and 1 mM ThDP was mixed 1:1 with the solution of 60 mM pyruvate (A) or 500 mM pyruvamide (B). The fluorescence changes were measured with a 305 nm cutoff filter (excitation wavelength is 295 nm). Solid curves (shown in lighter color) represent the best fit (A) with the single-exponential with the steady-state equation, A_1 = 0.214, k_1 = 2.62 s^{-1}, and k_{lin} = 0.0025 V/s, and (B) with double-exponential equations, A_1 = 0.033, k_1 = 0.173 s^{-1}, A_2 = 0.19, and k_2 = 0.015 s^{-1}.

cence are best fitted to a double-exponential equation with a linear component. The faster rate constant (responsible for the lag phase in fluorescence quenching) was not well defined above 15 mM pyruvate; hence, we could not determine whether it had reached saturation with pyruvate (inset to Figure 8). The value of the slower rate constant (k_{fluo}) did not change much if the data were fitted to a single-exponential equation with a linear component, providing that the curve was truncated to omit the lag phase. The rate constant of the fluorescence quenching (k_{fluo}), corresponding to the major change in fluorescence, exhibited hyperbolic dependence on pyruvate concentration (Figure 8) and was fitted to eq 3. The rate constant upon saturation with pyruvate is 6.3 s^{-1}, and the half-saturation concentration of pyruvate is 41.2 mM. The offset of the curve is 0.152 s^{-1}; however, due to its low value, this parameter has a large relative error and can be omitted without significantly changing the remaining parameters (Table 4). Utilization of the Hill equation with or without an offset did not change the results of the fit since the value of the Hill coefficient is near unity (Table 4). We calculated a monotonically decreasing function for the upper limit of pyruvate consumption in the course of the fluorescence experiments on the basis of (a) the activity v_1 of the maximally active enzyme form E_1 and (b) the time required for the experiment, as deduced from the rate constant of fluorescence change. For the lowest pyruvate concentration (1.5 mM) utilized in the fluorescence experiment, 5.3% pyruvate conversion was calculated, while for a concentration >5 mM, less than 1% of pyruvate is consumed. The actual amount of pyruvate depleted is expected to be much less than those values since v_1 represents the maximally attainable rate.

When pyruvamide was used in place of pyruvate, the fluorescence quenching behavior could be described by a two-exponential equation (Figure 7B), with both phases being

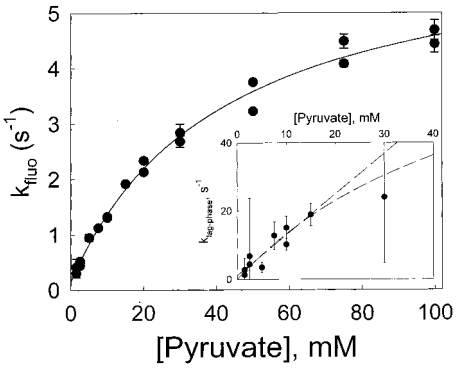

FIGURE 8: Pyruvate-dependent fluorescence changes in WT YPDC. All conditions are as in Figure 7. The progress curves for the fluorescence change on addition of different pyruvate concentrations were fitted to a double-exponential equation. The solid curve represents the best fit to the Michaelis−Menten equation with an offset and parameters $k_{on} = 6.3\ s^{-1}$, $K_d = 41.2$ mM, and $k_{off} = 0.15\ s^{-1}$. Inset: rate constant of the first relaxation. The solid curve represents the best fit to the hyperbolic equation ($k_{max} = 84.7\ s^{-1}$, $K_d = 53.6$ mM), and the dashed line represents the best fit to the linear equation ($k_{on} = 1.19\ mM^{-1}\ s^{-1}$, $k_{off} = 1.09\ s^{-1}$).

Table 4: Parameters of the Fluorescence Quenching Experiment[b]

k_{on} (s^{-1})	k_{off} (s^{-1})	K_d (mM)	n_H
6.13 ± 0.22	0.000[a]	34.9 ± 3.00	1.0[a]
6.26 ± 0.26	0.151 ± 0.080	41.2 ± 5.17	1.0[a]
7.32 ± 0.94	0.000[a]	53.7 ± 17.2	0.85 ± 0.07
4.86 ± 0.39	0.075 ± 0.209	47.6 ± 19.9	0.92 ± 0.20

[a] The parameter was fixed to the presented value. [b] Row 1, data were fitted to the Michaelis−Menten equation with no offset. Row 2, data were fitted to the Michaelis−Menten equation with offset. Row 3, data were fitted to the Hill equation with no offset. Row 4, data were fitted to the Hill equation with offset.

much slower than in the presence of pyruvate. The faster phase has an amplitude approximately 15% of the total fluorescence quenched, with a rate constant equal to 0.17 s^{-1} at 250 mM pyruvamide. The slower step was characterized by a 10-fold slower rate constant.

Circular Dichroism Kinetic Studies of Acetoin Formation by the E477Q Variant. The rate of formation of the carboligase side product acetoin by the E477Q variant at pH 5.1 was measured at 280 nm. The results revealed a marked effect of preincubation with pyruvate (Figure 9). When holoenzyme was exposed to a mixture of 10 mM pyruvate and 50 mM acetaldehyde, the rate in the initial part of the progress curve was 5.83 mdeg/min (0.83 unit/mg). However, the rate decreased to a new steady-state value of 2.03 mdeg/min (0.29 unit/mg) with a rate constant of transition equal to 0.26 min^{-1}. An estimate of the pyruvate concentration indicated that even after 30 min there remained sufficient substrate to saturate the acetoin-forming activity. "Activation" was also noticeable at the beginning of the curve, showing that in the presence of pyruvate the activity increases during the first several seconds, but, due to the manual mixing, neither the activity prior to activation nor the rate constant for the activation could be determined.

When the variant was preincubated with pyruvate and the reaction was initiated by the addition of acetaldehyde, the initial rate of acetoin formation was equal to 0.49 mdeg/min (0.069 unit/mg). This steady-state rate increased to 1.91 mdeg/min (0.27 unit/mg) with a rate constant of the transition equal to 0.24 min^{-1}.

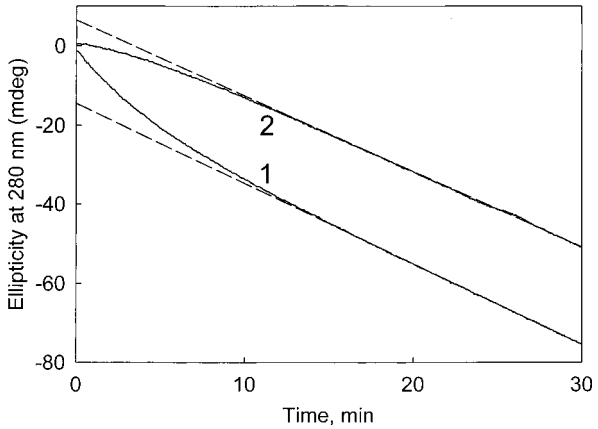

FIGURE 9: Effect of preincubation with pyruvate on scalemic acetoin formation by the E477Q variant of YPDC. The E477Q YPDC variant (0.194 mg/mL) was dissolved in the 50 mM acetate and 100 mM MES, pH 5.1, containing 5 mM $MgCl_2$ and 0.1 mM ThDP. It was either added to a reaction mixture containing 10 mM pyruvate and 50 mM acetaldehyde (curve 1) or preincubated for 5 min with 10 mM pyruvate to which was then added acetaldehyde to a final concentration of 50 mM (curve 2). The formation of scalemic acetoin was monitored by CD at 280 nm. The progress curves were fitted to eq 2 and resulted in the following parameters: (curve 1) $v_0 = 5.83$ mdeg/min, $v_1 = 2.03$ mdeg/min, and $k_{tr} = 0.26\ min^{-1}$; (curve 2) $v_0 = 0.486$ mdeg/min, $v_1 = 1.91$ mdeg/min, and $k_{tr} = 0.24\ min^{-1}$. Dashed lines represent asymptotic final steady states.

DISCUSSION

Need To Reexamine the Activation of Yeast Pyruvate Decarboxylase. We undertook a study of the activation of the E477Q variant to determine which of the explanations proposed in a previous paper (*15*) could explain the hyperbolic steady-state kinetics observed at low pH. We expected the progress curve for acetaldehyde formation to be either linear or linear with an initial lag phase. The observed progress curves had a lag phase; however, the slope of the linear portion decreased during the course of the reaction, resulting in curves with an inflection point (Figure 1). The mathematical treatment requires two exponentials with a linear part. One may have tried to explain the observations invoking two pre-steady-state steps prior to achieving steady state. However, an essential element of this kinetic mechanism is that a transient intermediate can be formed in a single-turnover process, and (a) it can be depleted (as in the case of the E477Q variant and the WT YPDC at low pH) or (b) it can persist (as in the case of WT YPDC at most pH values) during the pre-steady state. The molar extinction coefficient for this intermediate at 340 nm is about 8000 $M^{-1}\ cm^{-1}$ for the E477Q variant (Figure 1) and 41000 $M^{-1}\ cm^{-1}$ for WT (Figure 2). No intermediate in the reaction shown in Scheme 1 is expected to have such a high extinction coefficient at 340 nm. Nor can the observation be explained by a pre-steady-state consumption of pyruvate, since this would require depletion of 700 μM pyruvate by only 0.35 μM enzyme, clearly not consistent with single turnover. Discounting these options, the logical manner in which to treat the data is to assume the occurrence of transient changes in the steady-state rate of product formation. However, by definition, the steady-state rate cannot change; rather, the apparent change in steady-state rates is likely the result of a transition of the enzyme from one conformation to another with a different steady-state rate. The rate constant for the

second transition (k_{tr2}) was lower than the k_{cat} for either the E_1 or the E_2 state, which dictates that the step responsible for the transition be excluded from the catalytic cycles of the E_1 and E_2 states and also provides a valid premise for considering those states as discrete steady states. On the time scale of the transition k_{tr2}, the E_1 state is expected to have an unchanging molar ratio of the intermediates in the catalytic cycle. The same considerations are expected to hold for the E_2 state. As a result, the rate of product formation will report the change in total concentrations of the E_1 and E_2 states rather than the relative distribution of various intermediates in these states.

To our surprise, WT YPDC displayed progress curves with the same shape at pH $\leq$5.0 and at high pyruvate concentrations (Figure 2). Detailed analysis of the progress curves for WT YPDC revealed that, for a broad range of pH values, two transitions were present and only the steady-state rates were subject to change. This suggested the existence of three enzyme conformations (denoted as E_0, E_1, and E_2) characterized by three distinct steady-state rates (v_0, v_1, and v_2) and connected by two steps (i.e., $E_0 \rightarrow E_1 \rightarrow E_2$).

The scenario that the observed shape of the progress curves is due to inactivation of the enzyme at pH below 5.0 was ruled out by a comparison of the enzyme activity in the stock solution before and after the experiment, showing that the enzyme is stable at all pH values studied. In fact, the enzyme is much more stable at lower than at higher pH, the reason for excluding data acquired at pH 7.0. Additional evidence that the decrease of the rate is not an artifact could be deduced from the data themselves. Were the observed changes in activity due to inactivation of the enzyme, the posttransitional activity would be expected to asymptotically approach zero. The possibility that pyruvate has an adverse effect on the enzyme, indirectly causing its inactivation, was ruled out as follows. The rate constant for the step responsible for the decrease in activity (k_{tr2}) exhibited saturation with pyruvate. The progress curve presented in the inset of Figure 2 shows that, at sufficiently high pyruvate concentration, the activity decrease is followed by an increase, not expected if simple inactivation by substrate is the reason for the loss of activity.

The previous model for YPDC activation predicted the presence of two enzyme states (*4*) on the basis of data at pH 6.0, and the resting state in the absence of substrate ("unregulated enzyme") was believed to have no activity. The transition between the two states was suggested to represent a slow reversible conformational change, after the obligatory substrate-binding step at a special regulatory site. Extensive site-directed mutagenesis studies performed in this laboratory have pointed to C221 as the residue at which activation of YPDC by substrate is triggered. The unexpected observation, revealing that variants substituted at position 221 (lacking the putative regulatory site) still possess activity equal to at least 25% of the fully activated enzyme, indicated that, even prior to the formal activation, YPDC might be active. The recent study, carried out in this laboratory in collaboration with the Halle group, showed that under some circumstances the C221A variant also displays a lag phase in the progress curves, attributed to a slow pre-steady-state step independent of substrate binding (*12*).

Our data for the E477Q variant and WT YPDC provide the basis for further modifications in the model for activation. The dramatic changes in the relative steady-state activity of the E_1 and E_2 states, giving rise to S-shaped progress curves at low pH, leave no doubt that at least one additional transient enzyme state and one additional transition are present on the pathway to the final state. Although the shape of the progress curves at pH 6.0 resembled the previously reported one, the presence of two transitions was evident even at this pH. The cumulative data for all pH values and the persistence of the trend in the changes in parameters with changes in pH, in our view, provide convincing evidence for their existence at all pH values studied.

Analysis of the Three Steady States and the Transitions Connecting Them. (A) The First Enzyme Conformation (E_0) Appears To Be Inactive. In principle, in addition to the relaxations pertinent to YPDC, a relaxation associated with the coupling enzyme used in the assay may be expected with a rate constant equal to $V_{max}/K_{m(P)}$ [where V_{max} is the number of units of the coupling enzyme (units/mL = mM/min) added and K_m is its Michaelis constant for the product assayed] (*19*). However, the transient associated with the coupling enzyme (in this case, ADH) will always be independent of the concentration of pyruvate, the substrate of the principal reaction. Also, due to the sequential nature of the coupled assay and the initial concentration of the assayed product being zero, the rate prior to the first intrinsic transition may be artificially reduced and appear to be zero. In the discussion below, we assume that the E_0 state is inactive and acknowledge that further studies will be needed to definitively establish the validity of this assumption.

(B) The First Transition in the Progress Curves Corresponds to a Substrate-Binding Step. The rate constant of this transition (k_{tr1}) varies linearly with pyruvate concentration, suggesting that the observed transition coincides with a substrate-binding step. From the slope of the line and its intersection with the ordinate axis, the rate constants for complex formation (k_1) and breakdown (k_{-1}), respectively, can be calculated. The rate constant for complex formation k_1 is faster at low pH, whereas the rate constant for complex breakdown (k_{-1}) is virtually independent of pH (Table 3). Should this step correspond to substrate binding in the regulatory site, the forward rate would be expected to have the opposite pH dependence, since at lower pH there would be a smaller fraction of $C221S^-$, the reactive species at the regulatory site (*7*). Hence, were the regulatory site involved, the rate constant for the forward reaction should decrease with decreasing pH.

Since the only binding sites for pyruvate on WT YPDC monomer are the regulatory and active sites, we are compelled to suggest that the pyruvate molecule responsible for the first transition binds in the active site. Thus, the increasing rate constant with decreasing pH for enzyme−substrate complex formation may reflect on the protonation of carboxyl groups of either the pyruvate molecule or the active site residues D28 or E477, the two negatively charged residues in close proximity to the incipient 2-α-lactyl-ThDP (LThDP). This substrate-binding step is a necessary but is not a sufficient condition for the transformation of E_0 to E_1, since if this were the only step responsible for the transformation, once the acetaldehyde product is released, the enzyme would revert to the nonactive E_0 state. In the earlier model it was assumed that a slow conformational step separates activated and unregulated enzyme forms. The slow

rate of this step ensured that activated enzyme may undergo multiple catalytic turnovers upon activation, thus exhibiting hysteresis. In the present study, the rate constant of the first transition is faster than the turnover number of the resulting state, at least at low pH. To illustrate the point, k_{on} of the first transition at pH 4.5 is 197 M^{-1} s^{-1}, resulting in an apparent rate constant of 10 s^{-1} at 50 mM pyruvate. This value is larger than k_{cat} of the E_1 state (5.9 s^{-1}); hence, the E_0 and E_1 states are not separated from each other kinetically.

Our recently developed alternating sites mechanism for YPDC (see Scheme 2) can resolve the dilemma without additional assumptions. According to this mechanism, the unliganded dimer of the E_0 state is converted to doubly liganded dimer of the E_1 state, and the alternating sites mechanism would ensure that at no point does the catalytic cycle return to a unliganded state (see below).

(C) The First Transition in the Progress Curves Reports the Initiation of the Alternating Sites Mechanism. In a recent paper we presented supporting evidence for the proposition that activated YPDC (corresponding to the E_2 state in this paper) adheres to an alternating sites mechanism (*16*). Our proposed structural model involves interaction of the active sites in a functional ("tight") dimer and is based on the asymmetry of the functional dimer being perpetuated through the catalytic cycle.

The activation phenomenon was proposed to involve major conformational changes in the YPDC tetramer, converting a symmetric tetramer to an asymmetric one (*20*). In the course of these conformational changes, the structure of the functional dimer itself and the intersubunit interface between the two monomers in the dimer are preserved, and the major changes involve the interface between two functional dimers in the tetramer. Therefore, unregulated YPDC is likely to utilize the alternating site mechanism, just as its activated counterpart.

As mentioned above, the resting enzyme (E_0) in the absence of substrate exists predominantly in some type of symmetric conformation, similar to the one observed in the crystal structures (*1*, *2*) or in solution (*21*). Both active sites of this enzyme conformation are characterized by a disordered state of two flexible loops, 104−113 and 290−304 (*1*, *2*). Therefore, the histidines at positions 114 and 115, flanking one of the loops and implicated in substrate binding, even in the best case could only provide a dysfunctional binding site for pyruvate. Additional constraint may be imposed by disoriented loop(s) blocking the entrance to the active site. Therefore, binding of substrate in an active site of an asymmetrical conformation of YPDC might exhibit very low affinity.

The k_{on} for the first transition must be compared with the steps of catalysis first order in substrate. In steady-state kinetic terms, those steps are represented by the k_{cat}/K_m ratio. The k_{on} rate constant of the first transition (k_1 in Table 3) is at least 10 times smaller than k_{cat}/K_m of the first active enzyme conformation E_1 (Table 1) at all pH values. Also, k_1 displays a pronounced pH dependence, whereas k_{cat}/K_m is pH independent (Table 1), suggesting that the transition step (k_{tr1}) itself cannot be part of the catalytic cycle in the E_1 state.

Additional insight as to which steps might be involved in the transformation of the E_0 to E_1 state was provided by fluorescence data. Previously, it was hypothesized that the intrinsic fluorescence changes of YPDC probably originate from the interaction of W493 and F502 residing on two neighboring subunits of the functional dimer (*1*), suggesting that global structural changes could be monitored by fluorescence quenching studies. In addition, it was reported from this laboratory that W412, located in the active site near ThDP, does not contribute to the intrinsic YPDC fluorescence quenching caused by the conformational changes. For example, variants substituted at the 412 position displayed the same fluorescence quenching upon binding of ThDP as did WT YPDC (*11*).

Addition of pyruvate to the WT YPDC holoenzyme led to a rapid quenching of the fluorescence. At low pyruvate concentration a lag phase could be discerned in the progress curves. This lag phase was ill-defined above 15 mM pyruvate concentration, preventing us from further characterizing it with respect to a substrate-binding step. However, the presence of step(s) prior to the step responsible for fluorescence quenching is quite clear. The rate constant for fluorescence quenching exhibited saturation with pyruvate concentration, and therefore, these changes must be preceded by a substrate-binding step. The apparent dissociation constant for the substrate-binding step has a surprisingly high value of 41.2 mM (Table 4).

The rate constant of fluorescence quenching has values intermediate between those for the two transitions observed in the progress curves of product formation. Both the values of the rate constants and their dependence on substrate concentration make it tempting to propose that it is the binding step observed through the rate constant k_{tr1} which initiates the fluorescence changes. However, the K_{d1} value determined from k_{tr1} as the ratio of the rate constants k_{-1}/k_1 is equal to 1.61 mM at pH 4.5, 25 times lower than the one observed in fluorescence quenching experiments. A possible explanation is that the apparent rate constant k_{tr1} describes a step after the substrate-binding step with extremely low affinity. Were this the case, the slope of the k_{tr1} vs [S] (rate constant k_1) would actually be equal to the k_{on}/K_d, where K_d is dissociation constant of the enzyme−substrate complex and k_{on} and k_{-1} are the forward and reverse rate constants for transformation of this complex. In this case, k_{-1}/k_1 would characterize the overall equilibrium, including both the binding and the transformation steps. A low value of k_{-1}/k_1 compared to the K_d determined from fluorescence studies would suggest that the equilibrium of the second step shifted in the direction of the transformed complex.

Setting K_d equal to 41.2 ± 5.2 mM, the value determined in the fluorescence quenching experiments, results in the rate constant k_{on} = 8.1 ± 1.3 s^{-1} at pH 4.5. Fitting to different equations resulted in a broader range for K_d equal to 31.9−70.9 mM, leading to a value of k_{on} in the range of 6.1−14.4 s^{-1}. This value is similar to the rate constant obtained from fluorescence quenching (see Table 4) and, what is more meaningful, to the k_{cat} value of the E_1 enzyme form (see Table 1). Due to the presence of additional transition steps, no higher concentrations of pyruvate could be utilized in acetaldehyde-forming experiments at pH 4.5. On the other hand, due to the fast consumption of pyruvate at higher pH values, we were also limited to pH 4.5 in the characterization of the pyruvate concentration dependence of fluorescence quenching.

One could argue that binding of pyruvate might take place in the regulatory site, and the pH dependence is misleading because a noncovalent complex rather than a hemithioketal is formed at this step. Indeed, the increasing affinity with decreasing pH might be explained through protonation of H92, C221S$^-$, or/and pyruvate. However, formation of a simple noncovalent YPDC−pyruvate complex would hardly explain its effect on the enzyme because of the requirements imposed on pyruvate to bridge two residues on two domains. In a recent paper, an alternative residue R224, rather than C221, was suggested to participate in binding the regulatory pyruvate molecule, on the basis of an X-ray structure of YPDC saturated with 300 mM pyruvamide (*22*). However, careful examination of the interactions of the YPDC with pyruvamide revealed that pyruvate is highly unlikely to bind at that location (*16*). As will be discussed in the later section (titled YPDC Possesses Multiple Active Forms and Activation Pathways), pyruvate and pyruvamide have different activation pathways, which could be explained through distinct binding sites. We therefore favor the alternative, according to which the first transition reflects binding of the substrate in the active site. Additional support for the notion that the regulatory site is not involved in the first transition is discussed in the next section.

(D) The Second State (E_1) Depicts the Active Conformation of the "Unregulated" Enzyme. If the first transition corresponded to binding of substrate in the active site, it would result in the enzyme state (E_1) formerly considered unregulated. As discussed above, this enzyme form is expected to conform to the alternating sites mechanism. The substrate-dependent rate was best described by a Michaelis−Menten equation at all pH values. This may appear contradictory to the idea that the two active sites of the dimer act in a mutually interdependent manner. However, in the alternating sites model, the substrate-binding steps for two active sites are separated by an irreversible step, resulting in the visibility of only a single binding step. It can be demonstrated that if the symbol E in the alternating sites model (Scheme 2) corresponds to unregulated enzyme, then the steady-state rate is hyperbolic and is well accounted for by the equation:

$$v = \frac{V_{max}S}{K_m + S} \tag{4}$$

where

$$V_{max} = \frac{k_{c1}(k_{c2} + k_{c4})k_{c5}}{k_{c1}k_{c4} + k_{c1}k_{c5} + k_{c2}k_{c5}}$$

$$K_m = \frac{k_{s1}k_{c1}(k_{c2} + k_{c4} + k_{s4})k_{c5} + k_{s2}k_{s3}k_{c2}k_{c5}}{k_{s1}k_{s3}k_{c1}k_{c4} + k_{s1}k_{s3}k_{c1}k_{c5} + k_{s1}k_{s3}k_{c2}k_{c5}}$$

$$V_{max}/K_m = \frac{k_{s1}k_{s3}k_{c1}(k_{c2} + k_{c4})}{k_{s1}k_{c1}(k_{s4} + k_{c2} + k_{c4}) + k_{s2}k_{s3}k_{c2}}$$

The rate constants correspond to those in Scheme 2. The steps involving SES intermediates, and implicated in the substrate inhibition, are omitted for simplicity.

The initial rate of the E_1 state allows us to conclude that the regulatory site is not involved in the functioning of this state. Were binding of substrate in the regulatory site a prerequisite for catalysis, sigmoidal v_0−[S] curves would have resulted.

The maximal rate of the E_1 state increases more than 30-fold with a pH increase from 4.5 to 6.5. A similar 29-fold increase was observed in K_m, resulting in a pH-independent k_{cat}/K_m for the E_1 state in the pH range of 4.5−6.5, suggesting that there is no change in total charge in the rate-limiting step of the reaction in the *V*/*K* regime. Perhaps, the rate-limiting step is a pH-independent conformational change, as was concluded in the previous section. Consistent with the idea that the E_1 state represents unregulated enzyme form, the *V*/*K* plots for BFD (a related enzyme not subject to substrate activation) also appear to be pH independent from pH 5.0 to pH 8.0 (*23*). Since both enzymes exhibit an alternating sites mechanism, it is reasonable to deduce that the rate-limiting step for the *V*/*K* regime is a conformational change for both enzymes.

Additional insight can be gleaned from an inspection of the equation for V_{max}, K_m, and V_{max}/K_m of the E_1 state. The simplest set of conditions that will lead to the observed effect of pH on those parameters is $k_{s4} \ll (k_{c2} + k_{c4})$ and $k_{s1}k_{c1}(k_{c2} + k_{c4}) \gg k_{s2}k_{s3}k_{c2}$ at all pH values. If k_{c2} and k_{c4} were to increase with increasing pH, both V_{max} and K_m would increase, whereas the V_{max}/K_m would be pH independent. The inequality $k_{s4} \ll (k_{c2} + k_{c4})$ means that consumption of the SEN intermediate in the forward direction (through the catalytic cycle) is much faster than reversal of substrate binding and LThDP formation. The condition $k_{s1}k_{c1}(k_{c2} + k_{c4}) \gg k_{s2}k_{s3}k_{c2}$ is more complicated to analyze due to involvement of several substrate-binding and catalytic steps. It is instructive to consider two limiting cases: $k_{c2} \gg k_{c4}$ and $k_{c2} \ll k_{c4}$. If $k_{c2} \gg k_{c4}$, then $k_{s2}/k_{s1} \ll k_{c1}/k_{s3}$. The rate constants k_{s1} and k_{s3} are likely to include both binding of pyruvate and LThDP formation, and therefore a small rate constant for the binding step may be compensated for by a large rate constant for LThDP formation. The ratio k_{s2}/k_{s1} is the kinetic equivalent of the dissociation constant of the first active site, while the ratio k_{c1}/k_{s3} is the kinetic dissociation constant of the second active site, implying that the first active site has a higher apparent affinity than the second active site. In the second case, when $k_{c4} \gg k_{c2}$, one cannot draw such simple conclusions, and the kinetic dissociation constants may have an inverse relationship if k_{c2} is small enough compared to k_{c4}.

As discussed above, WT YPDC has highly coupled decarboxylation and product release, resulting in a single step k_R (Scheme 3). The initial rate of the unregulated enzyme is well accounted for by the Michaelis−Menten equation with the parameters:

$$V_{max} = k_R$$

$$K_m = \frac{k_{s4} + k_R}{k_{s3}} \tag{5}$$

$$V_{max}/K_m = \frac{k_{s3}k_R}{k_{s4} + k_R}$$

Accordingly, the conditions for V_{max}/K_m being constant simplified to $k_{s4} \ll k_R$, with the same implication as above.

The K_m of the E_1 state is pH independent between pH 5.0 and pH 6.0 but changes dramatically outside this range,

decreasing 10-fold with a pH decrease to 4.5 and increasing 3−4-fold with a pH increase from 6.0 to 6.5. The change at low pH may reflect titration of pyruvate or of one of the two residues, D28 or E477, below pH 5.0, whereas the change above pH 6.0 may be a consequence of titration of one of two active site histidines implicated in the binding of pyruvate.

The rate constant for fluorescence quenching at saturation with pyruvate (6.3 s^{-1}) is similar to the k_{cat} of the E_1 state. Therefore, it is possible that the step responsible for fluorescence quenching is a part of the catalytic cycle, and it is the rate-limiting step under saturation with substrate. Intermediates preceding the rate-limiting step accumulate in much higher concentration than intermediates after it, which should result in the accumulation of the highly fluorescent intermediates, contrary to our observations. However, the alternating sites mechanism could explain this apparent contradiction. The transformation of SEN to EN (Scheme 2) starts with a postdecarboxylation intermediate in one active site of the functional dimer and terminates with a postdecarboxylation intermediate in the second active site. As was postulated earlier (*16*), two subunits of the asymmetric functional dimer have conformations suitable for two different phases of the reaction: pre- and postdecarboxylation. In the course of the reaction, the conformations of the subunits in the functional dimer are interchanged. First of all, this interchange of the conformations does not change the overall conformation of the tetramer and, therefore, will not result in a change in fluorescence. Most probably, the conformational change proceeds through the symmetric tetramer conformation, and this step might be rate limiting for both (a) first entering the catalytic cycle and (b) proceeding through it. Therefore, it is reasonable to suggest that the step converting the symmetric to an asymmetric tetramer is the same one that is responsible for the fluorescence quenching, and it is rate limiting under saturation with substrate.

(E) The Second Transition Likely Involves Binding in the Regulatory Site. The second transition exhibited saturation with substrate, and therefore it corresponds to a transformation of an enzyme−substrate complex. In the course of this transformation, the steady-state rate of the complex changes, resulting in a relaxation observed in the progress curves. Both forward and reverse rate constants for this transformation and the K_d value of the enzyme−substrate complex were determined from k_{tr2} (Table 3).

Both active sites of the functional dimer are involved in the catalytic cycle and are already occupied in the E_1 state prior to the second transition. It was previously found (*15*) that the pyruvate molecule cannot access the active site once it is occupied by pyruvate or by any ThDP-bound covalent intermediate. This per se leads to the conclusion that the active site may not be involved in the second transition, pointing to the regulatory site as the most likely alternative pyruvate-binding site.

The forward rate constant (k_2) for the transformation of the enzyme−substrate complex is pH independent, implying that, prior to the slow step reflected in the second transition, not only binding of pyruvate in the regulatory site but also formation of the hemithioketal has taken place. The rate constant for the reverse step (k_{-2}) is very small, rendering the second transition almost irreversible. The K_d for the enzyme−substrate complex decreases with decreasing pH, perhaps indicative of the neutralization of the negative charge of pyruvate. The pyruvate anion might be difficult to bind near C221S$^-$; however, the positive charge of H92 (*7*) will assist binding, and this side chain may also undergo titration in this pH range, resulting in higher affinity for pyruvate at lower pH values.

At pH 6.0, the K_d is 20 mM, much larger than the estimated kinetic dissociation constant (K_a) of the regulatory site (*16*). However, the kinetic dissociation constant also includes the rate constants of all other steps on the pathway to a functioning enzyme. If the binding step and the transformation step were the only steps present, the K_a would be expected to equal 0.59 mM, similar to that determined in the steady-state experiments. The large standard deviations of the parameters render it impossible to predict whether other reversible steps are present on the pathway leading from the E_1 to the E_2 state.

The apparent rate constant for the second transition (k_{tr2}) displayed substantial inhibition by substrate, especially at higher pH (see Figure 6). As a logical extension of the alternating sites mechanism, one would expect the asymmetry of the subunits in the functional dimer to pertain not only to active sites but to the regulatory sites as well. Preliminary X-ray structural evidence points to an interaction of the negative charges in the C221D and C221E variants with H92 in only two of four subunits (Arjunan, Wei, et al., in preparation). Were only two of the four regulatory sites per tetramer occupied for optimal conformation, binding of substrate in the two remaining regulatory sites could lead to suppression of the rate. The pronounced effect of pH could reflect that the pK_a values of the two C221 residues involved in the activation are lower than the pK_a values of the remaining two C221 residues.

(F) The Third State (E_2) Corresponds to the Enzyme Form Usually Referred to as "Activated". This enzyme state was extensively characterized using steady-state kinetic experiments. The E_2 state exhibited cooperativity, and the data were therefore fitted to the Hill equation. All of the parameters of the Hill equation varied with pH (Table 2).

The V_{max} increased 55-fold with a pH increase from 4.5 to 6.5. The $S_{0.5}$ showed only a moderate 5.5-fold increase in the same pH range; it was unchanged between pH 5.0 and pH 6.0 and slightly decreased below and increased above this range, as did the K_m of the E_1 state. Therefore, the same explanations may apply here, and the less pronounced pH dependence may reflect the fine-tuning of the YPDC that took place during the second transition.

Both ratios that relate to the rate-limiting step in the predecarboxylation phase, $V_{max}/S_{0.5}$ and $V_{max}/S_{0.5}^n$ (for more details on the meaning of those parameters, see ref *16*), are bell-shaped with the optimum near pH 5.5. The pH dependence of either of these ratios suggested that at least two acid−base groups with pK_a values within or near the pH range utilized are involved in the rate-limiting step in the predecarboxylation phase of the reaction. At all pH values except pH 4.5 the catalytic efficiency of the E_2 state was higher than of the E_1 state, affirming that the second transition brings further improvement to the active enzyme. However, the same transition results in a deterioration of the catalytic efficiency at pH 4.5.

(G) The Hill Coefficient of the E_2 State Varies with pH. The Hill coefficient changes from 0.72 at pH 4.5 to 1.43 at pH 6.5. Negative cooperativity was previously observed in this laboratory for the C221S variants of YPDC (*6*) but never before for the WT enzyme. Previously, positive cooperativity of YPDC was explained in a number of ways. The traditional model of YPDC activation relied on *ordered binding* first in the regulatory and then in the active site, and activity originated only from the latter site (*24*). The alternative explanation recently introduced proposes that the positive cooperativity is the result of a concerted mode of action of two interacting monomers in the same conformation in each dimer (*22*). Neither previous model could predict negative cooperativity. On the other hand, an alternating sites model with *random order of substrate binding* to regulatory and active sites could give rise to either negative or positive cooperativity (*16*). In this model, substrate may bind to an active site prior to binding in the regulatory site, as seen for the E_1 state.

The values of the Hill coefficient determined here are much smaller than those determined in steady-state experiments (*14*). For example, at pH 6.0, the Hill coefficient is 1.37 for the E_2 state. The same enzyme preparation utilized in this study gave a Hill coefficient of 1.6−1.7 at pH 6.0 in the steady-state experiments. The most likely explanation is that in the current study the states with different activities are resolved in the fitting procedure, whereas in the steady-state experiments the progress curve is assumed to be a linear function. The rate constant k_{tr2} is quite small even at saturation with substrate. For the second transition to be completed to an extent of 95%, the time required will be given by $\ln(20)/k_{tr2} \approx 3/k_{tr2}$. And, since k_{tr2} is a monotonically increasing function, the completion time will be a monotonically decreasing one, equal to 50 s at 1 mM pyruvate and 15 s at 20 mM pyruvate. With the $S_{0.5}$ near 1 mM at pH 6.0, pyruvate concentrations of 0.1 mM or lower would be needed for the rate measurements. Values of k_{tr2} corresponding to those concentrations will be much smaller than those in Figure 6, resulting in hundreds of seconds of data acquisition. Low values of $S_{0.5}$ are indeed observed at low pH values, perhaps leading to larger errors in the value of the Hill coefficient.

Another complicating factor is that the slower the rate constant for the transition, the longer the time required to ascertain that the lag phase has been completed. A further difficulty is that the longer data acquisition time at low pyruvate concentrations would result in a greater extent of substrate consumption, leading to an artificially decreasing rate with increasing time, the opposite of the observed activation phenomenon leading to an increasing rate. Under these conditions, the progress curves would appear linear long before the lag phase has been completed. Therefore, the lower the pyruvate concentration, the more artificially reduced is the steady-state rate of YPDC, resulting in the appearance of the higher degree of cooperativity than really exists. The above deficiencies result in the Hill coefficient being routinely overestimated in the steady-state studies, especially at low pH values. One way to avoid this dilemma is to acquire full progress curves and fit them to eq 1.

YPDC Possesses Multiple Active Forms and Activation Pathways. Both the first and second states (E_0 and E_1) correspond to the phenomenologically unregulated enzyme with unoccupied regulatory site. As was previously demonstrated in this laboratory, all variants substituted at the C221 position (and therefore unable to form a thiohemiketal complex) have significant activity. Therefore, C221 variants might be more similar to the E_1 state than to the activated enzyme. The hyperbolic substrate-dependent kinetic behavior of the E_1 transition appears to support this notion. One apparent discrepancy is the values of K_m for the E_1 state, always larger than K_m of the C221 variants, except at very low pH. At pH 4.5 the value of K_m decreased to 2.9 mM, comparable to those observed with the C221 variants. Undoubtedly, at higher pH the C221 residue of the WT YPDC exists mostly in its thiolate form, thus reducing the similarity with the C221A or C221S variants.

The E_2 state is the one usually considered to be the activated conformation of YPDC. However, at pH 4.5 and high pyruvate concentrations, additional transitions became apparent. The general conclusion in this study is that while the rate constants of the transitions change as a function of pH or pyruvate concentration, the very existence of these transitions under all conditions examined is clear. Consequently, those additional transitions are likely to exist at other pH values as well. This raises the issue of whether E_2 is the "final" state, similar to the active state in vivo, or are there some other states, which by virtue of their slow appearance cannot be characterized in the experiments carried out so far.

The transitions observed in the CD experiments support the idea that, in addition to the three states observed in the pre-steady-state kinetic study, there are some others that have distinct features. Those states of YPDC may be the ephemeral result of the alternating sites mechanism. Alternatively, they may represent stable conformations induced by binding a ligand in either the active or regulatory site. Some of the conformations are stable enough to be crystallized, such as those obtained in the presence of ketomalonate (*25*) or pyruvamide (*20*, *22*).

(A) Activation Pathways May Be Different for the Pyruvate- and Pyruvamide-Activated YPDC. Since 1978, pyruvamide has been accepted as an appropriate mimic of the effect of pyruvate on the activation pathway of YPDC. In an earlier paper we observed steady-state inhibition by pyruvamide, particularly pronounced with the D28-substituted variants (*15*). Those variants were also extremely sensitive to inhibition by pyruvate, with pyruvate and pyruvamide inhibiting in a synergistic manner. In light of those data, the pyruvamide molecule observed in the active site of YPDC (*24*) may actually represent the inhibitory mode of binding rather than mimicking substrate binding, thus raising the question whether it is relevant to the structure of activated YPDC. It is likely that the observed structure is more similar to the E_1 than to the E_2 state, due to involvement of an active site rather than a regulatory site.

This study presents one further indication that pyruvamide is not a perfect mimic for the activation process observed with pyruvate. In the presence of 250 mM pyruvamide (the concentration that presumably saturates the regulatory site of YPDC), the time course of fluorescence quenching was biphasic. The rate constant of the faster phase was 0.17 s^{-1}, nearly 40-fold smaller than the value of k_{fluo} in the presence of pyruvate (6.3 s^{-1} at saturation with pyruvate). The second rate constant that was responsible for 85% of the fluorescence

quenching was 0.015 s^{-1}, much slower than any transient process observed in the presence of pyruvate. In view of these results, although pyruvamide might be utilized to induce one of the alternative conformations of YPDC (see below), its use to study all facets of the activation phenomenon is now questionable.

(B) Acetaldehyde Induces a Different Conformation Than Pyruvate. The kinetics of acetoin formation by the E477Q variant at pH 5.1 monitored by circular dichroism demonstrated that acetaldehyde induces a state distinct from the one observed in the presence of pyruvate. Preincubation of the E477Q variant with pyruvate resulted in low acetoin-forming activity, which increased upon addition of acetaldehyde (curve 2 in Figure 9). The rate constant of this transition (0.004 s^{-1}) was slower than any other rate constant observed in the principal reaction.

The rate of acetoin formation at saturating acetaldehyde concentration depends on the concentration of the enamine intermediate and the rate constant for acetoin release from butanediol−ThDP. Earlier we demonstrated that the enamine protonation step is rate limiting for acetaldehyde formation by the E477Q variant (*15*), whereas acetoin release is rate limiting in the direction of acetoin formation (*16*). This ensures that all active sites of the E477Q variant are occupied by the enamine, both in the presence and in the absence of acetaldehyde. Therefore, the observed transition corresponds to a change in the rate of acetoin release.

Acetaldehyde formation is significantly suppressed in the presence of exogenous acetaldehyde (*26*). Thus, the higher rate of acetoin formation may result from the same conformation that exhibits the lower rate of acetaldehyde production. It is likely that YPDC preincubated with pyruvate accumulates a conformation suitable for acetaldehyde production. Addition of acetaldehyde induces conformational changes toward the conformation with high acetoin- and low acetaldehyde-forming rates. We recently observed a CD signature for this conformation on the E477Q variant of YPDC (negative peak centered at 320−330 nm), which linked it to other ThDP-dependent enzymes with carboligase-type activity, clearly supporting the above conjecture (*27*), This conformation might be important for yeast cells at high acetaldehyde concentrations to divert YPDC to acetaldehyde consumption. An earlier report that the acetaldehyde-binding site responsible for the transformation has very low affinity (*26*) suggests that 50 mM acetaldehyde may not be sufficient to saturate this site and that the final steady-state rate (dashed lines in Figure 9) would most probably correspond to a mixture of the enzyme in both conformations.

Stivers and Washabaugh demonstrated that when acetoin is formed from acetaldehyde as a sole substrate, only two binding sites are visible in initial rate curves (*28*). At the same time, it was previously demonstrated (*29*) that acetaldehyde binds in the regulatory site and can activate YPDC, suggesting that acetoin might also be formed according to the alternating sites mechanism, making one of the three required binding steps invisible.

It is possible that other compounds unrelated to the YPDC reaction may induce additional conformations, distinct from the ones observed here. For example, 0.1 M citrate commonly utilized for buffering of the YPDC assay resulted in a 2-fold decrease of the rate constant of YPDC fluorescence quenching by pyruvate when compared with the triple buffer (data not shown). The presence of four citrate molecules at the intersubunit interface of ZmPDC (*30*) and its effect on $K_{m(pyruvate)}$ for that enzyme (*31*) support the idea that pyruvate decarboxylases from other sources may also follow the same pattern.

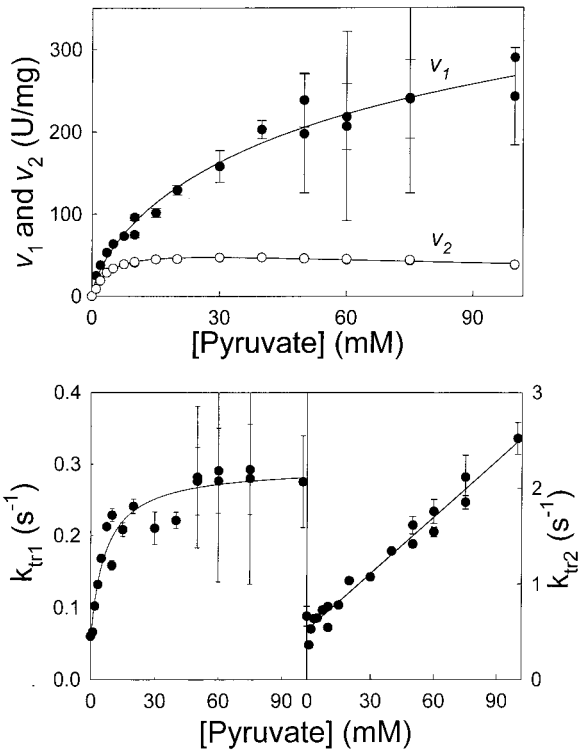

FIGURE 10: Alternative fit ($k_1 < k_2$) of the pH 6.0 WT YPDC data. Data were the same as utilized in Figure 6. The values of v_1 and v_2 were fitted to Hill and hyperbolic equations and the values k_{tr1} and k_{tr2} to a hyperbolic equation with an offset and to a linear equation. Solid curves represent the best fit with the following parameters: (v_1) k_{cat} = 500 s^{-1}, $S_{0.5}$ = 81.4 mM, and n_H = 0.72; (v_2) V_{max} = 57.7 units/mg, $S_{0.5}$ = 3.8 mM, n_H = 1.14, and K_i = 234.7 mM; (k_{tr1}) k_{on} = 0.245 s^{-1}, k_{off} = 0.052 s^{-1}, and K_d = 6.86 mM; (k_{tr2}) k_{on} = 19.6 M^{-1} s^{-1} and k_{off} = 0.52 s^{-1}.

(C) Sequence of Events in the Activation Pathway. As with most pre-steady-state kinetic data, there is uncertainty about the assignment of the apparent rate constants to the actual sequence of events. To illustrate, we present alternative treatments of the same data collected at pH 6.0, the only difference being reversal of the constraint of $k_1 > k_2$ to $k_1 < k_2$, leading to quite different sets of parameters (Figure 10). Although both sets of results appeared satisfactory a priori, we strongly favor the results of the former fit (presented in Figure 6) for the following reasons. With the second approach, the E_1 state was characterized by negative cooperativity and an unreasonably high k_{cat} of 500 s^{-1} per subunit. The parameters of the E_2 state did not change except that the Hill coefficient was close to unity. Activity of the E_2 state was 10-fold lower than of the E_1 state. This suggests that, for the condition $k_1 < k_2$, it would be more advantageous for the E_2 state of YPDC to have the lower activity. It is also difficult to accept the idea that the first transition would follow a substrate-binding step, whereas the second one would coincide with a substrate-binding step.

Another reason for selecting the fitting results presented in Figure 6 is based on our assumption that several conformational states may coexist even in unliganded enzyme, and binding of a ligand (or some other interactions,

Scheme 5: Random Pathway Mechanism

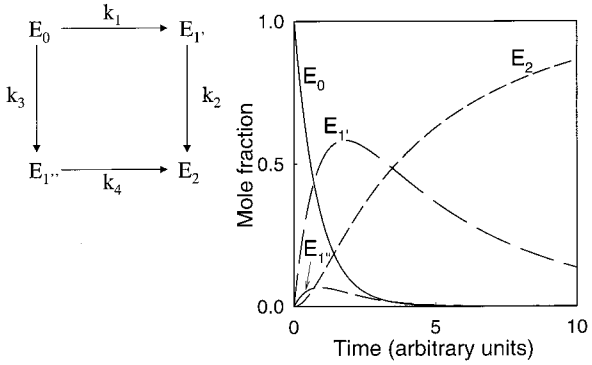

such as crystal packing forces) just makes some of these states more abundant. As a consequence, the two transitions occur in random order. It is notable that the three states observed in the progress curves must be formed in a sequential fashion. Were they formed in a branched reaction $E_1 \leftarrow E_0 \rightarrow E_2$, then only one transition would be observed, with a rate constant equal to the sum of the rate constants of the two branches.

The simplest model for a random pathway is presented in Scheme 5, in which the species E_0 has a choice of following a pathway either through $E_{1'}$ or through $E_{1''}$. The $E_{1'}$ state corresponds to unregulated enzyme with alternating sites and $E_{1''}$ would be equivalent to the activated enzyme without the alternating sites mechanism. The time-dependent changes in the concentrations of the $E_{1'}$ and $E_{1''}$ states are described by eqs 6A and 6B, respectively.

$$E_{1'} = \frac{k_1 E_{0(t=0)}}{k_1 + k_3 - k_2} \exp(-k_2 t) + \frac{k_1 E_{0(t=0)}}{k_1 + k_3 - k_2} \exp[-(k_1 + k_3)t] \quad (6A)$$

$$E_{1''} = \frac{k_3 E_{0(t=0)}}{k_1 + k_3 - k_4} \exp(-k_4 t) + \frac{k_3 E_{0(t=0)}}{k_1 + k_3 - k_4} \exp[-(k_1 + k_3)t] \quad (6B)$$

In the random model, with completely independent events, two of the four rate constants are redundant (since $k_1 = k_4$ and $k_2 = k_3$). However, this condition is not critical for our further consideration. It is possible that since both transitions appear to lead the enzyme in the same direction, the rates of the second step in each branch may be accelerated due to positive homotropic interactions. Let us assume that the rate constant for the reaction $E_0 \rightarrow E_{1'}$ (and $E_{1''} \rightarrow E_2$) is much larger than that for the step $E_0 \rightarrow E_{1''}$ (and $E_{1'} \rightarrow E_2$), that is, $k_1 \gg k_2$. Taking into consideration the equalities $k_1 = k_4$ and $k_2 = k_3$ leads to the simplification of eq 6 to those in eqs 7A and 7B.

$$E_{1'} = E_{0(t=0)}(1 - e^{-(k_1+k_3)t}) - E_{0(t=0)}(1 - e^{-k_2 t}) \quad (7A)$$

$$E_{1''} = E_{0(t=0)}(1 - e^{-(k_1+k_3)t}) - E_{0(t=0)}(1 - e^{-k_1 t}) \quad (7B)$$

It can be shown that both pathways have equal rates of formation of both $E_{1'}$ and $E_{1''}$.

The maximal transient concentrations of $E_{1'}$ and $E_{1''}$ would be dictated by the rate of reactions converting $E_{1'}$ and $E_{1''}$ into E_2. The faster one will result in the intermediate on this pathway (in the particular case intermediate $E_{1''}$) being present at only negligible concentrations, as illustrated in Scheme 5, where the rate constant k_1 is just 5 times larger than k_2, leading to significantly reduced concentration of the $E_{1''}$ intermediate. This situation will be almost indistinguishable from the simple reaction $E_0 \rightarrow E_{1'} \rightarrow E_2$, unless the physical property measured (activity, fluorescence, etc.) for intermediate $E_{1''}$ is much more pronounced than that same property for intermediate $E_{1'}$.

Therefore, with the condition of very different rate constants, one pathway will be much more populated in the measured property, and the other one's influence will be negligibly small. However, when the two rate constants have similar values, both pathways will contribute to the measured property and the actual state might be a mixture of several states. In most instances the rate constants k_{tr1} and k_{tr2} were well separated, and therefore there was only one predominant intermediate state. However, the danger that the E_1 state is actually a mixture of two states $E_{1'}$ and $E_{1''}$ was a real one. The substrate concentration dependence may allow us to demonstrate that the E_1 state corresponds to a single entity. The presence of more than one state would result in an apparent negative cooperativity. At all pH values the E_1 state was characterized by a simple hyperbolic substrate dependence, confirming that the E_1 state corresponded to one actual enzyme form.

(D) Mechanism of Alternating Sites and Activation-like Phenomena. The E_1 state displayed an important characteristic of the alternating sites mechanism of YPDC. Both active sites of the functional dimer are involved in the full catalytic cycle of the enzyme, but the initial rate is a hyperbolic function of substrate concentration. Therefore, *observation of hyperbolic steady-state kinetic behavior of WT YPDC or its variants does not necessarily mean that the active sites act independently of each other during catalysis.*

Another very important feature of the alternating sites mechanism is an observation that some step(s) leading from free enzyme is (are) not included as a part of the catalytic cycle. Therefore, a relatively slow rate of any of the steps not involved in the catalytic cycle may result in an activation-like phenomenon with a lag phase in the progress curves. For example, if substrate-binding and/or LThDP formation in the first active site (included in the step $E \rightarrow ES$ in Scheme 2) is slow, one would expect to see a lag phase. One of the major predictions of the alternating sites mechanism is that, under optimal conditions, the decarboxylation step in one active site is tightly coupled with product release from the second active site (Scheme 3). This condition will add the decarboxylation step $ES \rightarrow EN$ to the list of steps not included in the catalytic cycle and will potentially give rise to a lag phase.

Earlier, we suggested that involvement of the regulatory site facilitates the transition between symmetric and asymmetric conformations of YPDC but may not be essential to maintain the catalytic cycle (*16*). In fact, any interaction that promotes the transition may result in the activation phenomenon of YPDC. For example, the substrate mimic pyruvamide may "activate" YPDC due to its inhibitory mode of binding in the active site (*22*), simply by inducing and

Scheme 6: Sturctural Similarity of BFD, ZmPDC, and YPDC

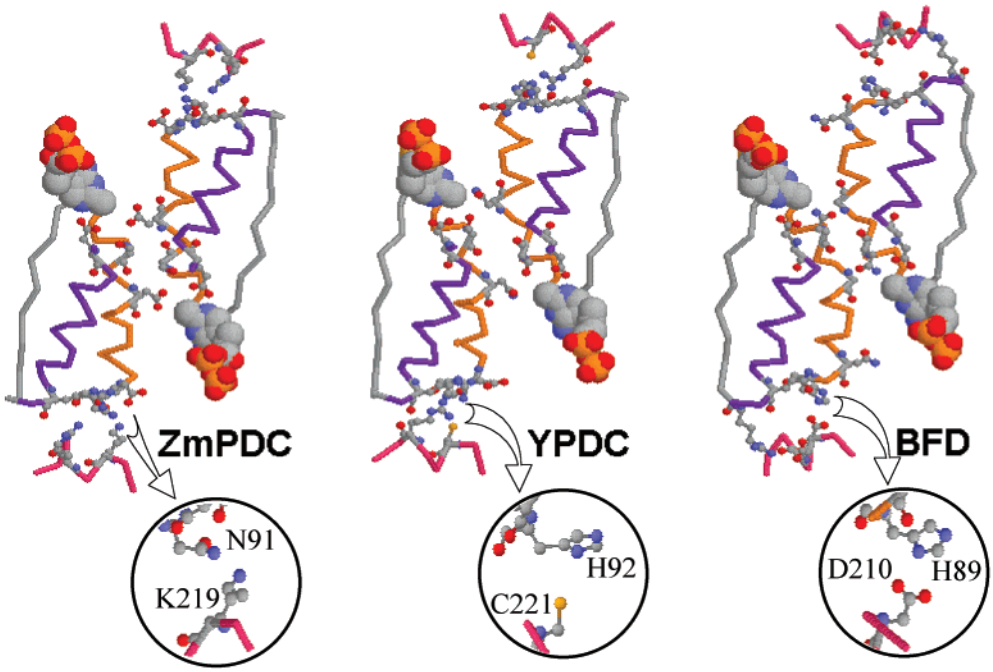

stabilizing an asymmetric conformation of YPDC.

An activation-like phenomenon with the characteristic lag phase was also observed with the plant pyruvate decarboxylase, where no regulatory site could be identified (*32*), perhaps signaling that this enzyme also utilizes the alternating sites mechanism with its plurality of possibilities for producing lag phases. Unfortunately, the three-dimensional structure of that enzyme is not yet available to test our hypothesis. For the available structures, however, we can deduce that other ThDP-binding enzymes may also utilize the alternating sites mechanism. For example, we recently characterized BFD and demonstrated that it also utilized an alternating sites mechanism (*33*). Comparison of the structures of three ThDP-dependent enzymes, YPDC, ZmPDC, and BFD, shows that all of them have an astonishing degree of similarity in the organization of their overall architecture of the α domains (Scheme 6). Not only are α-helixes preserved with the short interconnections from one subunit to another but also a critical interaction between the α and *β* domains (loops belonging to the *β* domain are shown in rose color). In the YPDC this critical interaction is C221 complexed with pyruvate and bridging to H92 of the α domain. In ZmPDC it is a hydrogen bond between K219 and N91, while in BFD it is an ion pair between D210 and H89. This may explain why the latter two enzymes do not require formal activation via a distinct regulatory site, as is the case with YPDC. On the basis of this strong similarity of the structure of the three enzymes, two of which have already been demonstrated to possess an alternating sites mechanism, we are tempted to suggest that ZmPDC may also adopt the same mechanism. Perhaps, if ZmPDC could be crystallized in the presence of pyruvamide, one could even observe an asymmetric state of that enzyme.

CONCLUSIONS

Although there might be some uncertainty as to the correct assignment of the observed transitions, there is no doubt concerning the presence of both transitions at all pH values studied. The substrate-dependent behavior of the rate constants for those transitions affirms that two different sites are involved in the expression of those steps. The first transition was assigned to the binding of substrate in the active site of the unregulated enzyme. The slow step resulting in the appearance of the transition is assigned to the enforcement of asymmetry in the functional dimer, a property that is central to the alternating sites mechanism. The second transition resulted in the formally activated enzyme with the regulatory site occupied. Additional transitions were noticed at low pH and high pyruvate concentration, as well as in the presence of acetaldehyde in the acetoin-forming carboligase reaction. It is also possible that many more transitions of YPDC actually exist and that neither of the enzyme states here described corresponds to the enzyme form that is active in the yeast cells. Acetaldehyde certainly induces a distinct conformation of YPDC, with a lower rate of acetaldehyde formation and an increased rate of acetoin production. However, most likely, even in the presence of acetaldehyde, the YPDC still adheres to the alternating sites mechanism. It is also noteworthy that additional conformational changes were observed in apo-YPDC upon binding of ThDP and Mg(II) (*34*), supporting our contention that this enzyme is a very important model for enzyme regulation in general.

REFERENCES

1. Dyda, F., Furey, W., Swaminathan, S., Sax, M., Farrenkopf, B., and Jordan, F. (1993) *Biochemistry 32*, 6165−6170.
2. Arjunan, P., Umland, T., Dyda, F., Swaminathan, S., Furey, W., Sax, M., Farrenkopf, B., Gao, Y., Zhang, D., and Jordan, F. (1996) *J. Mol. Biol. 256*, 590−600.
3. Boiteux, A., and Hess, B. (1970) *FEBS Lett. 9*, 293−296.
4. Hübner, G., Weidhase, R., and Schellenberger, A. (1978) *Eur. J. Biochem. 92*, 175−181.
5. Zeng, X., Farrenkopf, B., Hohmann, S., Dyda, F., Furey, W., and Jordan, F. (1993) *Biochemistry 32*, 2704−2709.
6. Baburina, I., Gao, Y., Hu, Z., Jordan, F., Hohmann, S., and Furey, W. (1994) *Biochemistry 33*, 5630−5635.

7. Baburina, I., Moore, D. J., Volkov, A., Kahyaoglu, A., Jordan, F., and Mendselsohn, R. (1996) *Biochemistry 35*, 10249−10255.
8. Baburina, I., Li, H., Bennion, B., Furey, W., and Jordan, F. (1998) *Biochemistry 37*, 1235−1244.
9. Baburina, I., Dikdan, G., Guo, F., Tous, G. I., Root, B., and Jordan, F. (1998) *Biochemistry 37*, 1245−1255.
10. Li, H., Furey, W., and Jordan, F. (1999) *Biochemistry 38*, 9992−10003.
11. Li, H., and Jordan, F. (1999) *Biochemistry 38*, 10004−10012.
12. Wang, J., Golbik, R., Seliger, B., Spinka, M., Tittmann, K., Hübner, G., and Jordan, F. (2001) *Biochemistry 40*, 1755−1763.
13. Wei, W., Liu, M., and Jordan, F. (2002) *Biochemistry 41*, 451−461.
14. Liu, M., Sergienko, E. A., Guo, F., Wang, J., Tittmann, K., Hübner, G., and Jordan, F. (2001) *Biochemistry 40*, 7355−7368.
15. Sergienko, E. A., and Jordan, F. (2001) *Biochemistry 40*, 7369−7381.
16. Sergienko, E. A., and Jordan, F. (2001) *Biochemistry 40*, 7382−7403.
17. Holzer, H., Schultz, G., Villar-Palasi, C., and Jutgen-Sell, J. (1956) *Biochem. Z. 327*, 331−344.
18. Ellis, K. J., and Morrison, J. F. (1982) *Methods Enzymol. 87*, 405−427.
19. Easterby, J. S. (1973) *Biochim. Biophys. Acta 293*, 552−558.
20. Lu, G., Dobritzsch, D., König, S., and Schneider, G. (1997) *FEBS Lett. 403*, 249−253.
21. Svergun, D. I., Petoukhov, M. V., Koch, M. H., and König, S. (2000) *J. Biol. Chem. 275*, 297−302.
22. Lu, G., Dobritzsch, D., Baumann, S., Schneider, G., and König, S. (2000) *Eur. J. Biochem. 276*, 861−868.
23. Weiss, P. M., Garcia, G. A., Kenyon, G. L., Cleland, W. W., and Cook, P. F. (1988) *Biochemistry 27*, 2197−2205.
24. Alvarez, F. J., Ermer, J., Hübner, G., Schellenberger, A., and Schowen, R. L. (1995) *J. Am. Chem. Soc. 117*, 1678−1683.
25. Furey, W., Arjunan, P., Chen, L., Sax, M., Guo, F., and Jordan, F. (1998) *Biochim. Biophys. Acta 1385*, 253−270.
26. Juni, E. (1961) *J. Biol. Chem. 236*, 2302−2308.
27. Jordan, F., Zhang, Z., and Sergienko, E. A. (2002) *Bioorg. Chem.* (submitted for publication).
28. Stivers, J. T., and Washabaugh, M. W. (1993) *Biochemistry 32*, 13472−12482.
29. Hübner, G., Fisher, G., and Schellenberger, A. (1970) *Z. Chem. 10*, 436.
30. Dobritzsch, D., König, S., Schneider, G., and Lu, G. (1998) *J. Biol. Chem. 273*, 20196−20204.
31. Bringer-Meyer, S., Schimz, K.-L., and Sahm, H. (1986) *Arch. Microbiol. 146*, 105−110.
32. Dietrich, A., and König, S. (1997) *FEBS Lett. 400*, 42−44.
33. Sergienko, E. A., Wang, J., Polovnikova, L., Hasson, M. S., McLeish, M. J., Kenyon, G. L., and Jordan, F. (2000) *Biochemistry 39*, 13862−13869.
34. Vaccaro, J. A., Crane, E. J., Harris, T. K., and Washabaugh, M. W. (1995) *Biochemistry 34*, 12636−12644.

BI011860A